Detailed magnetization study of quenched random ferromagnets. II. Site dilution and percolation exponents

S. N. Kaul* and P. D. Babu
School of Physics, University of Hyderabad, Central University P.O., Hyderabad-500 134, Andhra Pradesh, India
(Received 23 December 1993)

We report the experimental determination of the crossover exponent (ϕ) and the percolation critical exponents for magnetization (β_p) and spin-wave stiffness (θ) for quench-disordered (amorphous) three-dimensional ($d=3$) dilute Heisenberg ferromagnets. The values of ϕ, θ, and β_p, so obtained, as well as those of the percolation correlation-length critical exponent ν_p and the conductivity exponent σ, deduced from the exponent equalities $\nu_p=\phi-(\theta/2)$ and $\sigma=(d-2)\nu_p+\phi$, conform very well with the most accurate theoretical estimates published recently. A comparison of the presently determined exponent values with those theoretically predicted for site or bond percolation on a $d=3$ *crystalline* lattice asserts that the critical behavior of percolation on a *regular* $d=3$ lattice does not get altered in the presence of quenched randomness if the specific-heat exponent of the regular system is negative. Consistent with the Alexander-Orbach conjecture (Golden inquality), the fracton dimensionality $\bar{\bar{d}}$ of the percolating cluster at threshold (the conductivity exponent σ) turns out to be $\bar{\bar{d}}\simeq 4/3$ ($\sigma\leq 2$). The present results vindicate the universality hypothesis.

I. INTRODUCTION

Randomly diluted magnetic systems with short-range interactions have captured the attention of scientists worldwide in recent years because they provide a fertile testing ground[1,2] for percolation theories.[3,4] The most intriguing aspect of dilute magnetism is the behavior of such systems near the point $Q(p=p_c, T=0)$ in the $T_C(p)$ $\{T_N(p)\}$ phase diagram ($T_C\{T_N\}$ denotes the Curie {Néel} temperature, p is the concentration of magnetic atoms in a given ferromagnetic (FM) {antiferromagnetic (AF)} alloy series, and p_c is the critical concentration (percolation threshold) at which an infinite FM (AF) cluster first appears when p is increased from zero at $T=0$). The connectivity and thermal fluctuations become critical as the point Q is approached along the paths $p\rightarrow p_c$ at $T=0$ and $T\rightarrow 0$ at $p=p_c$, respectively. Along the former path, the spontaneous magnetization (percolation probability) M goes smoothly to zero while the correlation (connectedness) length ξ and susceptibility (mean cluster size) χ diverge in accordance with the relations[1,3,4]

$$M(T=0,p)=m_p(p-p_c)^{\beta_p}\ ,\quad p>p_c\ , \tag{1}$$

$$\xi(T=0,p)=\xi_p(p-p_c)^{-\nu_p}\ ,\quad p>p_c\ , \tag{2}$$

and

$$\chi(T=0,p)=\chi_p(p-p_c)^{-\gamma_p}\ ,\quad p>p_c\ . \tag{3}$$

In Eqs. (1)–(3), β_p, ν_p, and γ_p are the percolation critical exponents for M, ξ, and χ. Several numerical and analytic calculations[4,5] of the exponents for bond and site percolation on lattices of dimension d have yielded accurate values for $d=2$ only. For $d=3$, the theoretical estimates for β_p, γ_p, ν_p and the thermal-to-percolation crossover exponent $\phi=\nu_p/\nu_T$ (ν_T is the critical exponent for thermal correlation length), defined as[1,3,4]

$$T_C(p)=t_p(p-p_c)^{\phi}\ ,\quad p>p_c\ , \tag{4}$$

range between[2–5] 0.34 and 0.47, 1.71 and 1.82, 0.71 and 0.90, and 0.9 and 1.2, respectively. Early experimental determination of the percolation and thermal critical exponents for crystalline $d=2$ and $d=3$ Ising[6] and Heisenberg[7] dilute antiferromagnets revealed that the exponent values, not so accurate for $d=3$ as for $d=2$ systems, agree well with the theoretical estimates for $d=2$ dilute magnets only. While constant attempts are being made, on the theoretical side, to refine[4,5] the values of critical exponents for percolation on $d=3$ lattices, parallel efforts on the experimental front are lacking. One of the main reasons for this is the difficulty in finding crystalline magnetic systems that can be diluted without drastic changes in the lattice symmetry or in the lattice parameter. An effective way to tackle this problem is to choose dilute ferromagnets in the amorphous state instead. Dilute magnets with quenched disorder have long been regarded as model systems[8] for studying percolation phenomena and yet little or even no progress has been made in understanding their percolation behavior, as is evident from the following remarks. While the sole attempt[9] to experimentally determine the critical exponents β_p and γ_p for amorphous dilute ferromagnets is plagued with thermal-to-percolation crossover effects, all the theoretical approaches proposed hitherto treat site or bond percolation on a regular crystalline lattice and tacitly assume[1,4] validity of the famous Harris criterion, even for *extreme* disorder (i.e., for p just above p_c), in order to describe the critical behavior of quenched random site- or bond-diluted magnets. In this context, it should be recalled that the Harris criterion, in its original form, states that the *thermal* critical exponents of a pure (ordered) $d=3$ spin system do not get altered in the presence of *weak short-*

ranged quenched disorder if the specific-heat, C_p, critical exponent α of the pure system is *negative* and hence is strictly valid in the weak-disorder limit only.

This state of affairs prompted us to determine accurately the crossover exponent ϕ and the percolation critical exponents for magnetization, β_p, and for spin-wave stiffness, θ, defined as[1,3,4]

$$D(T=0,p)=d_p(p-p_c)^{\theta}\ ,\quad p>p_c\ , \tag{5}$$

for amorphous (a-) $(Fe_pNi_{1-p})_{80}(B,Si)_{20}$ (series I) and $(Fe_pNi_{1-p})_{80}P_{14}B_6$ (series II) alloys. The main reasons for choosing these alloy systems for the intended study are (i) Ni atoms in them carry a negligibly small moment[10] and hence act as magnetic dilutents, (ii) the thermal correlation length in (Ni-Fe)-metalloid glasses diverges at T_C even for compositions close[11] to $\tilde{p}_c$ [the Fe concentration at which paramagnetic (PM), ferromagnetic, reentrant (RE), and spin-glass (SG) phases coexist in the magnetic phase diagram], and (iii) the values of spin-wave stiffness directly measured by the inelastic neutron scattering technique equal[12] those deduced from the thermal demagnetization of $M(T,p)$ for all the compositions down to $\tilde{p}_c$ in similar (Ni-Fe)-based metallic glasses.

II. EXPERIMENTAL RESULTS AND ANALYSIS

The reader should refer to the preceding paper[13] (henceforth referred to as Paper I) for details concerning the sample preparation, compositional analysis, and magnetization measurements.

A. Magnetic phase diagram

Figures 1 and 2 depict the magnetic phase diagrams in the Fe concentration range $0\lesssim p\lesssim 0.625$ for the a-$(Fe_pNi_{1-p})_{80}(B,Si)_{20}$ (series I) and a-$(Fe_pNi_{1-p})_{80}P_{14}B_6$ (series II) alloys, respectively, obtained by accurately determining[10,14–19] T_C, T_{RE}, and T_{SG} from ac (zero-field) susceptibility $\chi_{ac}(T)$, electrical resistivity $\rho(T)$, and bulk magnetization (BM) measurements. In these diagrams,

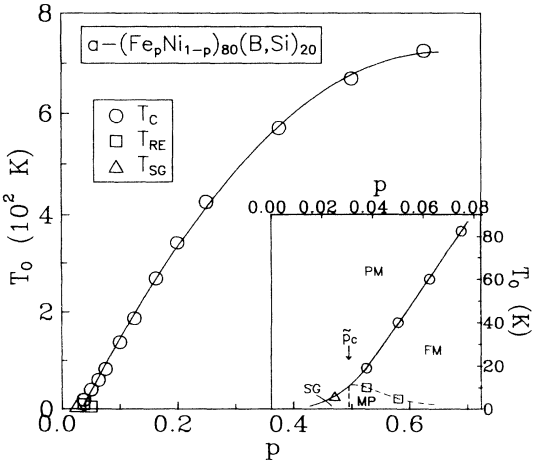

FIG. 1. Magnetic phase diagram on the Fe-poor side for amorphous $(Fe_pNi_{1-p})_{80}(B,Si)_{20}$ alloys. The uncertainty limits lie well within the size of the symbols.

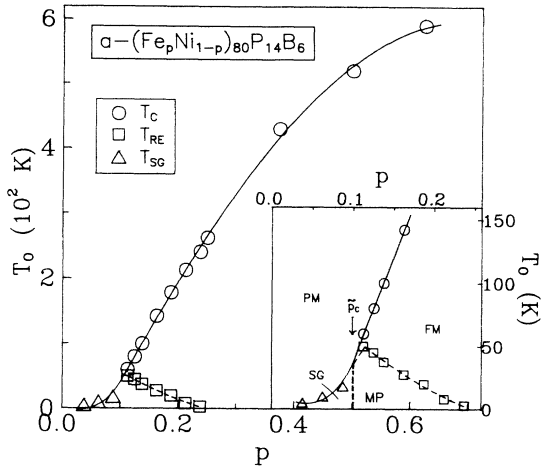

FIG. 2. Magnetic phase diagram on the Ni-rich side for amorphous $(Fe_pNi_{1-p})_{80}P_{14}B_6$ alloys. The uncertainty limits lie well within the size of the symbols.

T_C and T_{SG} denote the temperatures at which FM-PM and SG-PM phase transitions occur while T_{RE} ($\ll T_c$) marks the onset of strong irreversibility in the low-field ($H\lesssim 100$ Oe) magnetization. In other words, $T_{RE}(H)$ is the temperature at and below which the zero-field-cooled and field-cooled magnetizations corresponding to a given field strength H cease to possess the same value and $T_{RE}=\lim_{H\to 0}T_{RE}(H)$. Note that the Fe concentration at which PM, FM, RE, and SG phases coexist $\tilde{p}_c\simeq 0.03$ for series I and 0.10 for series II. As the temperature is lowered below T_C, the alloys with $p\gtrsim\tilde{p}_c$ enter at $T=T_{RE}$ into a mixed (reentrant) state in which long-range FM order coexists with the cluster spin-glass order. This inference regarding the nature of the RE phase is drawn from the observation that spontaneous magnetization does not drop to zero but instead remains finite as temperature is lowered through T_{RE} and that this nonzero spontaneous magnetization is accompanied by the thermomagnetic and thermoremanent effects which are normally associated with SG order. Moreover, there are strong indications that, unlike PM-FM and PM-SG phase transitions, the FM-RE transition [the dashed curves through $T_{RE}(p)$ data in Figs. 1 and 2] may not be a true phase transition in the thermodynamic sense. These findings are in conflict with the earlier claim[20] that the RE state in the same or similar alloy systems as the ones under consideration is a pure SG state and the FM-RE transition represents a well-defined FM-SG phase transition. Since the main concern of this paper is to ascertain whether or not the percolation theories correctly describe the observed variation of T_C with p in the vicinity of, but above, p_c, the nature of the RE phase and the transition at T_{RE} will form the subject of a forthcoming paper.

In order to accurately determine the thermal-to-percolation crossover exponent ϕ, we proceed as follows. Equation (4) can be rewritten in the form

$$t\equiv T_C(p)[dT_C(p)/dp]^{-1}=(p-p_c)/\phi\ . \tag{6}$$

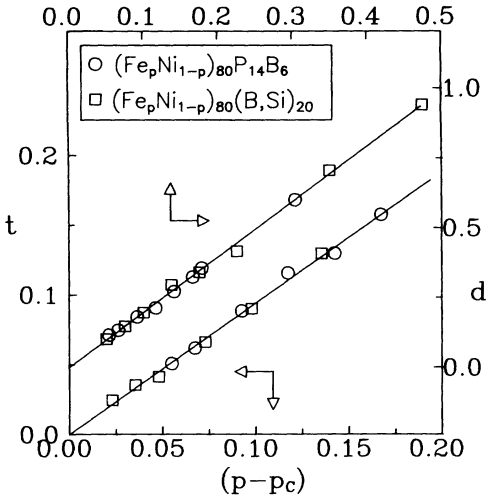

FIG. 3. Quantities $t \equiv T_C(p)[dT_C(p)/dp]^{-1}$ and $d \equiv D(T=0,p)[dD(T=0,p)/dp]^{-1}$ as functions of Fe concentration p in the amorphous $(Fe_pNi_{1-p})_{80}(B,Si)_{20}$ and $(Fe_pNi_{1-p})_{80}P_{14}B_6$ alloys. The solid straight lines through the data points denote the least-squares fits to the combined data based on Eqs. (6) and (8) with the choice of parameters given in the text. The size of the symbols denotes the uncertainty limits.

It is evident from Eq. (6) that for concentrations in the close proximity to p_c (i.e., in the asymptotic critical region, ACR), the t versus p plot should be a straight line with slope $(1/\phi)$ and the intercept on the p axis equal to p_c. The data presented in Fig. 3 testify to the validity of this analytic approach for both the alloy series in question. The best least-squares (LS) straight-line fits to the $t(p)$ data based on Eq. (6) yield the values $\phi=1.09(3)$ [1.06(3)] and $p_c=0.026(2)$ [0.070(2)] in the concentration range $0.012 \leq (p-p_c) \leq 0.174$ $[0.043 \leq (p-p_c) \leq 0.168]$ for series I [II]. The straight line fit in Fig. 3 represents the LS fit to the combined $t(p)$ data for both the alloy systems based on Eq. (6) with the choice of the exponent $\phi=1.08(3)$; p_c values for the series I and II are the same as quoted above. These values of p_c and ϕ are then used in Eq. (4) to compute the corresponding values of the critical amplitude t_p. The continuous curves through the $T_C(p)$ data points in Fig. 4 are arrived at when the values of p_c, t_p, and ϕ, determined by the above-mentioned analytic method, are used in Eq. (4).

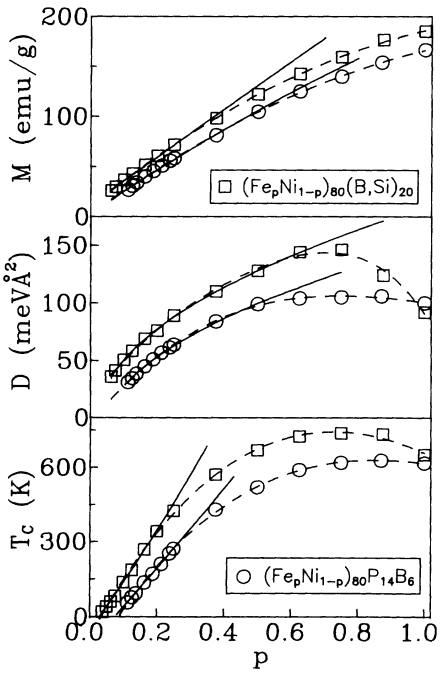

FIG. 4. $T_C(p)$, $D(T=0,p)$, and $M(T=0,p)$ as functions of Fe concentration p. The continuous curves through the data points represent the least-squares fits to the data based on Eqs. (4), (5), and (7) with the choice of parameters given in the text. The dashed curves serve to highlight the deviation of the data from the LS fits. The uncertainty limits lie well within the size of the symbols.

B. Spontaneous magnetization at 0 K

The magnetization (M) versus magnetic field (H) isotherm taken at 1.6 K in fields up to 20 kOe for a few representative compositions in the alloy series I is shown in Fig. 5. Similar M vs H curves are also obtained for various compositions in the alloy series II. Spontaneous magnetization at 0 K for different compositions in a given alloy series, $M(T=0,p)$, is obtained as an intercept on the ordinate when the linear high-field portion of the M vs H curve is extrapolated to $H=0$. Note that no distinction between the values of spontaneous magnetization at 1.6 and 0 K is made in this work. Another important point worth noting is that the M vs H isotherm at 1.6 K presents a slight curvature in the high-field region that persists to fields as high as 20 kOe (the curvature is more pronounced in series II than in series I) and a large[21]

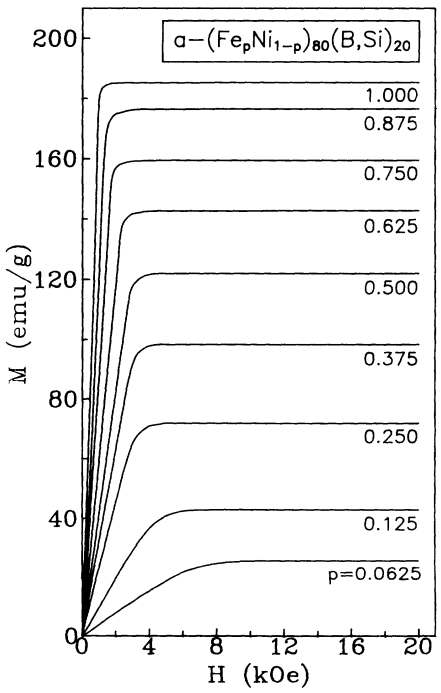

FIG. 5. Magnetization as a function of the external magnetic field at 1.6 K for a few representative compositions in the amorphous $(Fe_pNi_{1-p})_{80}(Bi,Si)_{20}$ alloy series.

high-field susceptibility ($\simeq 5\times10^{-5}$ emu/g Oe) particularly for the alloys with compositions just above $\tilde{p}_c$ (i.e., for $p-p_c \lesssim 0.06$), presumably due to the frozen cluster SG order embedded in a (long-range) FM matrix. The curvature increases progressively as $p\rightarrow\tilde{p}_c$. Such a curvature gives rise to undesirably large uncertainty in $M(T=0,p)$ for $p-p_c \lesssim 0.06$ if the above-mentioned extrapolation method is used. This problem is overcome by making the modified Arrott plot isotherm [$M^{1/\beta}$ vs $(H/M)^{1/\gamma}$], constructed out of the M vs H data taken at 1.6 K, linear, particularly in the high-field region, through a proper choice of the thermal critical exponents β and γ for the spontaneous magnetization and initial susceptibility. $M(T=0,p)$ is then computed from the intercept on the ordinate obtained by extrapolating the high-field linear portion of the modified Arrott plot isotherm to $(H/M)^{1/\gamma}=0$. The observed concentration dependence of $M(T=0,p)$ is displayed in Fig. 4. In the ACR, percolation theories[1,3,4] predict a variation of $M(T=0,p)$ with concentration of the form given by Eq. (1). An attempt to determine the critical exponent β_p from the

$$m(p)\equiv M(T=0,p)[dM(T=0,p)/dp]^{-1}$$

data using the analytic method described earlier in connection with the $t(p)$ data did not succeed for the following reason. The plot of m vs p exhibits marked curvature and hence the values β_p and p_c depend on the range of p used for the fit. A curvature in the m vs p plot evidently implies that the ACR for $M(T=0,p)$ is extremely narrow compared to that for $T_C(p)$ and that the correction-to-scaling (CTS) terms make significant contribution for concentrations not too close to p_c. In order to verify this assertion, the expression

$$M(T=0,p)=m_p(p-p_c)^{\beta_p}[1+a(p-p_c)^{\Delta_1}], \qquad (7)$$

which includes the CTS term with coefficient a and exponent Δ_1, is fitted to the $M(T=0,p)$ data over different concentration ranges by the LS method. The range-of-fit analysis, in which the variation in the fitting parameters m_p, p_c, β_p, a, and Δ_1, if any, is monitored as more and more data points taken at p values far away from p_c are excluded from the fit, yields the best LS fits (continuous curves through the data in Fig. 4) corresponding to the choice of the parameters $m_p=90(3)$ [109(2)] emu/g, $\beta_p=0.41(2)$ [0.43(2)], $p_c=0.026(2)$ [0.070(2)], $a=1.95(5)$ [0.95(5)], and $\Delta_1=1.00(1)$ [1.00(1)] within the concentration range $0.037\le(p-p_c)\le0.22$ [$0.043\le(p-p_c)\le0.43$] for series I [II].

C. Spin-wave stiffness at 0 K

Accurate values of the spin-wave stiffness at 0 K, $D(T=0,p)$, shown in Fig. 4 for $p\lesssim0.625$, have been deduced from the in-field magnetization data through an elaborate data analysis (whose details are furnished in Paper I) which allows for the field-induced energy gap in the spin-wave spectrum, the temperature renormalization of the spin-wave stiffness, and the low-lying excitations that, besides the spin-wave excitations, contribute to thermal demagnetization. In order to determine the percolation exponent θ for the spin-wave stiffness, the same analytic method as the one already described in Sec. II A is employed, in that Eq. (5) is rewritten as

$$d\equiv D(T=0,p)[dD(T=0,p)/dp]^{-1}=(p-p_c)/\theta \qquad (8)$$

and the quantity d is plotted against $(p-p_c)$ in Fig. 3. An examination of Fig. 3 reveals that this approach is valid for the glassy alloys investigated. The best least-squares straight-line fits to the $d(p)$ data based on Eq. (8) yield the values $\theta=0.505(5)$ [0.509(5)] and $p_c=0.025(2)$ [0.071(2)] in the concentration range $0.038\le(p-p_c)\le0.6$ [$0.042\le(p-p_c)\le0.43$] for series I [II]. The solid straight line in Fig. 3 represents the best LS fit to the combined $d(p)$ data for both the alloy series based on Eq. (8) with the choice of the critical exponent $0=0.505(5)$ and p_c the same as mentioned above for series I and II. The values of the exponent θ and critical concentration p_c so obtained are then substituted in Eq. (5) to compute the corresponding values of the critical amplitude d_p for the two alloy systems. The continuous curves through the $D(T=0,p)$ data (open circles and squares) shown in Fig. 4 represent the theoretical variation arrived at by inserting the values of p_c, d_p, and θ, determined by the above-mentioned procedure, in Eq. (5).

Note that the values of $T_C(p)$, $M(T=0,p)$, and $D(T=0,p)$ for amorphous $(Fe_pNi_{1-p})_{80}(B,Si)_{20}$ and $(Fe_pNi_{1-p})_{80}P_{14}B_6$ alloys determined in this work are listed in Tables I and II of Paper I.

III. DISCUSSION

With a view to demonstrating that the values of the percolation exponents (amplitudes) ϕ, β_p, and θ (t_p, m_p, and d_p) determined by the method described in the previous section are true asymptotic values and highlighting the importance of the CTS term in the case of $M(T=0,p)$, the quantities $[T_C(p)/t_p]^{1/\phi}$, $[M(T=0,p)/m_p]^{1/\beta_p}$, and $[D(T=0,p)/d_p]^{1/\theta}$ are plotted against $(p-p_c)$ in Fig. 6. The important points that merit attention are (i) the $T_C(p)$, $M(T=0,p)$, and $D(T=0,p)$ data yield the same (within the uncertainty limits) value for p_c for a given alloy series, (ii) p_c is nearly three times smaller in series I than in series II, (iii) the asymptotic critical region, where Eqs. (1), (4), and (5) hold, is wide for $T_C(p)$ and $D(T=0,p)$ but extremely narrow for $M(T=0,p)$, and (iv) the CTS term in Eq. (7) has to be taken into account in order to arrive at the true asymptotic values of the critical exponent β_p and amplitude m_p from $M(T=0,p)$ data taken at concentrations not too close to p_c. The present values of p_c [$p_c=0.026(2)$ for series I and 0.070(2) for series II] lie well below the critical concentrations for bond and site percolation[1] for nearest-neighbor (NN) exchange interactions on the fcc lattice (which forms an adequate description[14,15] of the NN atomic configuration in the glassy alloys in question), $p_c^b=0.119$ and $p_c^s=0.195$, but compare favorably with the critical concentration for site percolation on the fcc lattice when the exchange interactions involve first (1), second (2), and third (3) nearest neighbors,[1] i.e., with

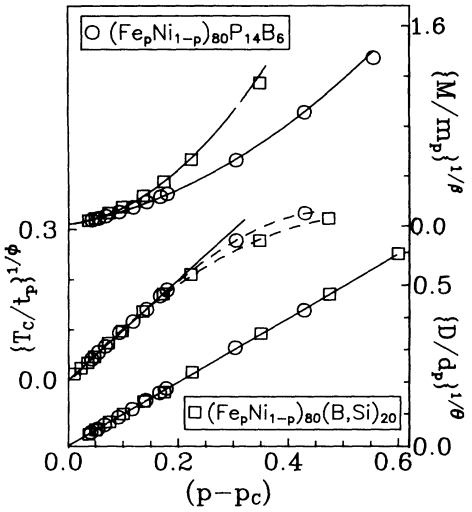

FIG. 6. Quantities $[T_C(p)/t_p]^{1/\phi}$, $[D(T=0,p)/d_p]^{1/\theta}$, and $[M(T=0,p)/m_p]^{1/\beta_p}$ as functions of Fe concentration p. The solid straight lines and curves through the data points represent the best least-squares fits to the data based on Eqs. (4), (5), and (7) of the text, while the dashed curves serve to highlight the deviations from the LS fits. The size of the symbols denotes the uncertainty limits.

$p_c^s(1,2,3)=0.061$. This comparison asserts that the range of exchange interaction in series II nearly equals the third NN distance (r_{3NN}) whereas exchange interactions in series I extend well beyond r_{3NN}.

The most intriguing, but still unresolved, aspect of percolation phenomena is the exact structure of the infinite cluster at and above p_c. This information is crucial to the understanding of most of the properties of random systems such as dilute ferromagnets, random resistor networks, microemulsions, and gels. Of all the model descriptions[2,22,23] of the infinite cluster structure proposed so far, the node-link model[23] due to Skal and Shklovskii and de Gennes (SSG) is by far the simplest one. According to this model, the crossover exponent ϕ, the spin-wave stiffness exponent θ, and the macroscopic conductivity (Σ) critical exponent σ [$\Sigma\sim(p-p_c)^{\sigma}$] are related to the critical exponents ν_p and ζ for the average distance between nodes [the percolation correlation or connectedness length, $\xi(T=0,p)\sim(p-p_c)^{-\nu_p}$] and the average length L of the one-dimensional random path between adjacent nodes [$L\sim(p-p_c)^{-\zeta}$] through the equalities[1-4,24],

$$\phi=\zeta=\nu_p/\nu_T\ , \tag{9}$$

$$\theta=2(\zeta-\nu_p)\ , \tag{10}$$

and

$$\sigma=(d-2)\nu_p+\zeta\ . \tag{11}$$

The presently determined values of the exponents ϕ and θ, when substituted in Eqs. (9)–(11), yield $\nu_p=\phi-(\theta/2)=0.84(3)$ [0.81(3)] and $\sigma=1.93(6)$ [1.87(6)] for series I [II] and $\nu_p=0.828(33)$ and $\sigma=1.91(6)$ for the combined data. The final values for the critical exponents of interest, i.e., $\beta_p=0.42(3)$, $\nu_p=0.83(3)$, $\phi=\zeta=1.08(3)$, $\sigma=1.91(6)$, and $\Delta_1=1.00(1)$, arrived at by taking into consideration all the sources of error, are in excellent agreement with the most accurate theoretical estimates $\beta_p=0.41(3)$, $\nu_p=0.87(7)$, $\phi=1.10(2)$, $\sigma=2.00(5)$, and $\Delta_1=1.1(2)$ for site or bond percolation on $d=3$ crystalline lattices reported[2,5,25-28] recently, and also with the experimental value[29] $\sigma=1.94(6)$ for water-in-oil microemulsion. Moreover, the values of the exponent ratios $\sigma/\nu_p=2.30(15)$ [2.31(16)] and 2.30(16) and $\beta_p/\nu_p=0.488(42)$ [0.531(45)] and 0.506(55) for series I [II] and the combined data conform very well with the recent theoretical estimates 2.276(12), 2.31(6), and 2.45(5) for σ/ν_p and 0.464(66) and 0.471(16) for β_p/ν_p obtained by finite-size scaling,[27] series expansion,[5,26] and Monte Carlo simulation,[30,31] while the values of the conductivity critical exponent σ for the investigated alloy series obey the inequality $\sigma\leq 2$ for $d=3$, due to Golden,[32] who assumed that the conducting backbone near p_c has a hierarchical node-link-blob structure.[22]

Within the framework of a model which is based on the assumption that the infinite cluster at p_c has a self-similar fractal structure[33] and makes use of the scaling arguments, the fractal dimension $\bar{d}$ and the spectral (fracton) dimensionality $\bar{\bar{d}}$ of the percolating cluster at threshold can be expressed in terms of the Euclidean dimension d and percolation critical exponents β_p, ν_p, and σ as[34,35]

$$\bar{d}=d-(\beta_p/\nu_p) \tag{12}$$

and

$$\bar{\bar{d}}=2(d\nu_p-\beta_p)/(\sigma-\beta_p+2\nu_p)\ . \tag{13}$$

Alexander and Orbach[34] conjecture that for percolation on the infinite cluster

$$\bar{\bar{d}}=\tfrac{4}{3} \tag{14}$$

independent of d. Substituting the exponent values determined in this work and setting $d=3$ in Eqs. (12) and (13), one obtains $\bar{d}=2.51(4)$ [2.47(5)] and 2.49(5) and $\bar{\bar{d}}=1.32(13)$ [1.31(13)] and 1.31(14) for series I [II] and the combined data. While the present values of fractal dimension are in excellent agreement with the Monte Carlo[31] and series expansion[36] estimates $\bar{d}=2.52(3)$ and 2.50(2), a comparison of our values for fracton dimensionality with Eq. (14) reveals that the present results are consistent with the Alexander-Orbach conjecture. Combining (13) and (14) and solving for σ yields the expression

$$\sigma=[(3d-4)\nu_p-\beta_p]/2\ . \tag{15}$$

For $d=3$, Eq. (15) reduces to $\sigma=(5\nu_p-\beta_p)/2$ and the presently determined values of ν_p and β_p when substituted in this relation give the values $\sigma=1.90(8)$ and 1.81(8) for the series I and II, which are the same (within the error limits) as those deduced from the relation, Eq. (11), predicted by the SSG node-link model.[23] Note that Eq.

(11) reduces to Eq. (15) if

$$\zeta=\bar{d}\nu_p/2 \tag{16}$$

and that Eq. (16), too, is satisfied in the present case. In view of the above observations, our results demonstrate that the SSG node-link, hierarchical node-link-blob, and self-similar fractal models are mutually consistent, even though these models differ widely in the microscopic details and hence form completely different descriptions of the structure of the infinite cluster at p_c. This is not surprising, considering that the structural details at length scales less than the correlation or connectedness length, $\xi(T=0,p)$, are of no consequence so long as $\xi(T=0,p)$ diverges at p_c. Thus Eqs. (9)–(11) and (15) have a universal character in that they are of more general validity than what an oversimplified underlying model would normally suggest. Other important points that deserve a mention at this stage are (i) a close agreement between the experimental values of the percolation critical exponents for amorphous site-diluted ferromagnets determined in this work and those theoretically predicted for site or bond percolation on three-dimensional crystalline lattices asserts that the critical behavior of percolation on a regular $d=3$ lattice remains unaltered in the presence of *quenched randomness* if the specific-heat critical exponent of the regular system is *negative*,[1,3,4] and (ii) the finding that the range of exchange interactions is widely different in the two alloy series and yet both the alloy series possess the same values for the percolation critical exponents vindicates the universality hypothesis. An inference like (i) above has recently been drawn based on the results of Monte Carlo simulations[37] of bond (site) percolation on random two-dimensional (three-dimensional) systems. Furthermore, consistent with the above observation (i), the results of electrical resistivity,[17,38] bulk magnetization,[17,18,39] and zero-field susceptibility[16,17,40,41] measurements [performed in the asymptotic critical region on the same or similar (Fe-Ni)-metalloid alloy systems as the present ones] have proved beyond any doubt the validity of the Harris criterion even for extreme disorder by unambiguously demonstrating that, even for compositions extremely close to (just above) $\tilde{p}_c$, T_C is sharply defined ($\Delta T_C/T_C \lesssim 10^{-4}$) and the asymptotic values of the thermal critical exponents for specific heat, spontaneous magnetization, and initial susceptibility are composition independent and the same as those theoretically predicted for an ordered three-dimensional ($d=3$) Heisenberg spin system.

Considering the fact that the critical concentration has not been approached sufficiently closely in the present experiments, a close agreement between experiment and theory might seem fortuitous, but the following observations do not support such an inference. In this context, it should be noted that the main difficulty in approaching p_c sufficiently closely in this work arises from the breakdown of long-range ferromagnetic order at $\tilde{p}_c$ (the concentration at which the present spin systems enter into a spin-glass state when the concentration p is lowered through $\tilde{p}_c$; see Figs. 1 and 2) which lies above p_c. The observations in question are (a) three different types of data [$T_C(p)$, $M(T=0,p)$, and $D(T=0,p)$] yield the same value for p_c for a given alloy series, (b) p_c is widely different in the two alloy series and yet both the alloy series yield identical values for the percolation critical exponents, and (c) within roughly the same concentration range, the need to include the correction-to-scaling term is felt only in the case of $M(T=0,p)$ but not for $T_C(p)$ and $D(T=0,p)$. On the other hand, one has to admit that the actual behavior of the investigated alloy systems is much more complicated than a simple dilution picture would normally suggest. This is so because the spin-glass phase exists for $p<\tilde{p}_c$ (and hence the SG order is present in the range $p_c \lesssim p \lesssim \tilde{p}_c$ also) and long-range ferromagnetic order breaks down before the percolation threshold p is reached. As a consequence, the magnetic atoms have a power-law (fractal) correlation near the percolation threshold if only the nearest-neighbor interaction is assumed. The Harris criterion is replaced by the Weinrib-Halperin criterion[42] which predicts new exponents even if $\alpha<0$ in the pure system. Thus, crossover to a new fixed point (critical behavior) is expected. The presence of spin interactions beyond the first neighbor in the systems under consideration should make the crossover spread out and new critical behavior hard to detect. This might offer a simple explanation for a seemingly wide critical region for $T_C(p)$ and $D(T=0,p)$ but certainly not for the necessity to include the CTS term only for $M(T=0,p)$. Moreover, there is no *a priori* reason to believe that one should obtain the pure values for the exponents in the crossover region. Furthermore, if the Weinrib-Halperin criterion[42] is applicable to the amorphous alloy systems studied in this work, the thermal critical exponents are also expected to possess values widely different from the pure ones for concentrations close to $\tilde{p}_c$. Extensive studies[16–18,38–41] of the thermal critical behavior in the alloys with p close to $\tilde{p}_c$, in which T_C has been approached sufficiently closely, do, however, yield the pure values for the thermal critical exponents. These contradictions can be laid to rest only when the type of measurements described in this work are performed on amorphous magnetic systems in which the formation of the spin-glass state at low concentrations can be completely avoided and long-range ferromagnetic order breaks down at p_c. Obviously, such a metallic alloy system is hard to realize in practice.

IV. SUMMARY AND CONCLUSIONS

High-resolution bulk magnetization, ac susceptibility, and electrical resistivity measurements have been performed on amorphous $(Fe_pNi_{1-p})_{80}(B,Si)_{20}$ and $(Fe_pNi_{1-p})_{80}P_{14}B_6$ alloys over a wide range of Fe concentration $0.025 \lesssim p \lesssim 0.625$ with a view to determining accurately the crossover exponent ϕ for $T_C(p)$ and the percolation exponents for magnetization (β_p) and spin-wave stiffness (θ). Reliable estimates have been obtained not only for these exponents but also for the correlation and conductivity exponents [deduced from the exponents θ, ϕ, and β_p with the aid of exponent equalities $\nu_p=\phi-(\theta/2)$ and $\sigma=(d-2)\nu_p+\phi$]. From the close

agreement between the values of crossover and percolation critical exponents ($\phi, \beta_p, \theta, \nu_p$, and σ) so obtained and those theoretically predicted for site or bond percolation on a $d=3$ crystalline lattice, we conclude that the critical behavior of percolation on a regular $d=3$ lattice remains *unaltered* in the presence of quenched randomness if the specific-heat exponent of the regular system is *negative*. The asymptotic critical region, where the single power-law behavior [i.e., Eqs. (1), (4), and (5)] is valid, is wide for $T_C(p)$ and $D(T=0,p)$ but extremely narrow for $M(T=0,p)$; in the latter case, the correction-to-scaling term in Eq. (7) had to be included in order to arrive at the true asymptotic value of the critical exponent β_p and amplitude m_p from $M(T=0,p)$ data taken at concentrations not too close to p_c. Consistent with the Alexander-Orbach conjecture (Golden inequality), the fracton dimensionality $\bar{\bar{d}}$ of the percolating cluster at threshold (the conductivity exponent σ) turns out to be $\bar{\bar{d}} \simeq \frac{4}{3}$ ($\sigma \leq 2$). Finally, the observation that the range of exchange interactions is widely different in the two glassy alloy series and yet the percolation critical exponents have the same values for both of them vindicates the universality hypothesis.

ACKNOWLEDGMENTS

Part of the work presented here was carried out at the Ruhr Universität Bochum, Germany, by one of the authors (S.N.K.) who thanks Professor S. Methfessel for providing the required experimental facilities. The financial support from the Department of Atomic Energy, India, under Project No. 37/10/93-G/6 is also gratefully acknowledged.

*Author to whom all the correspondence should be addressed.

[1]R. B. Stinchcombe, in *Phase Transitions and Critical Phenomena,* edited by C. Domb and M. S. Green (Academic, New York, 1983), Vol. 7, p. 151.

[2]L. J. de Jongh, in *Magnetic Phase Transitions,* edited by M. Ausloos and R. J. Elliott (Springer-Verlag, Berlin, 1983), p. 172; A. Coniglio, ibid., p. 195; Phys. Rev. Lett. **46**, 250 (1981).

[3]D. Stauffer, Phys. Rep. **54**, 1 (1979); J. W. Essam, Rep. Prog. Phys. **43**, 833 (1980).

[4]D. Stauffer and A. Aharony, *Introduction to Percolation Theory* (Taylor & Francis, Bristol, 1991).

[5]J. Adler, Y. Meir, A. Aharony, and A. B. Harris, Phys. Rev. B **41**, 9183 (1990), and references cited therein; T. C. Lubensky and J. Wang, ibid. **33**, 4998 (1986).

[6]R. A. Cowley, G. Shirane, R. J. Birgeneau, and E. C. Svensson, Phys. Rev. Lett. **39**, 894 (1977); R. A. Cowley, R. J. Birgeneau, G. Shirane, H. J. Guggenheim, and H. Ikeda, Phys. Rev. B **21**, 4038 (1980).

[7]R. J. Birgeneau, R. A. Cowley, G. Shirane, J. A. Tarvin, and H. J. Guggenheim, Phys. Rev. B **21**, 317 (1980); R. A. Cowley, G. Shirane, R. J. Birgeneau, E. C. Svensson, and H. J. Guggenheim, Phys. Rev. B **22**, 4412 (1980).

[8]Articles by D. J. Thouless, S. Kirkpatrick, and T. C. Lubensky, in *Ill-Condensed Matter,* edited by R. Balian, R. Maynard, and G. Toulouse (North-Holland, Amsterdam, 1979), pp. 1, 321, 405; L. S. Meichle and M. B. Salamon, J. Appl. Phys. **55**, 1817 (1984).

[9]P. Majumdar, S. M. Bhagat, and M. A. Manheimer, J. Magn. Magn. Mater. **54–57**, 271 (1986); J. Appl. Phys. **57**, 3479 (1985).

[10]S. N. Kaul, IEEE Trans. Magn. **MAG-17**, 1208 (1981).

[11]J. A. Tarvin, G. Shirane, R. J. Birgeneau, and H. S. Chen, Phys. Rev. B **17**, 241 (1978); M. B. Salamon and A. P. Murani, J. Appl. Phys. **55**, 1688 (1984).

[12]R. J. Birgeneau, J. A. Tarvin, G. Shirane, E. M. Gyorgy, R. C. Sherwood, H. S. Chen, and C. L. Chien, Phys. Rev. B **18**, 2192 (1978).

[13]S. N. Kaul and P. D. Babu, preceding paper, Phys. Rev. B **50**, 9308 (1994).

[14]S. N. Kaul, Phys. Rev. B **24**, 6550 (1981).

[15]S. N. Kaul, Phys. Rev. B **27**, 5761 (1983); **27**, 6923 (1983).

[16]S. N. Kaul, Phys. Rev. B **38**, 9178 (1988).

[17]S. N. Kaul and M. Sambasiva Rao, Phys. Rev. B **43**, 11 240 (1991) and J. Phys. Condens. Matter (to be published).

[18]S. N. Kaul, J. Magn. Magn. Mater. **53**, 5 (1985); IEEE Trans. Magn. **MAG-20**, 1290 (1984).

[19]S. N. Kaul, Solid State Commun. **36**, 279 (1980).

[20]Y. Yeshurun, M. B. Salomon, K. V. Rao, and H. S. Chen, Phys. Rev. B **24**, 1536 (1981); J. A. Geohegan and S. M. Bhagat, J. Magn. Magn. Mater. **25**, 17 (1981); M. A. Manheimer, S. M. Bhagat, and H. S. Chen, *ibid.* **38**, 147 (1983).

[21]S. N. Kaul and M. Rosenberg, Phys. Rev. B **27**, 5698 (1983).

[22]H. E. Stanley, J. Phys. A **10**, L211 (1977); A. Coniglio, *ibid.* **A15**, 3829 (1982).

[23]A. S. Skal and B. I. Shklovskii, Fiz. Tekh. Poluprovodn. **8**, 1582 (1974) [Sov. Phys. Semicond. **8**, 1029 (1975)]; P. G. de Gennes, J. Phys. (Paris) Lett. **37**, L1 (1976).

[24]T. A. L. Ziman, J. Phys. C **12**, 2645 (1979).

[25]D. J. Bergman, E. Duering, and M. Murat, J. Stat. Phys. **58**, 1 (1990).

[26]J. Adler, Y. Meir, A. Aharony, A. B. Harris, and L. Klein, J. Stat. Phys. **58**, 511 (1990).

[27]D. B. Gingold and C. J. Lobb, Phys. Rev. B **42**, 8220 (1990).

[28]E. Duering and H. E. Roman, J. Stat. Phys. **64**, 851 (1991).

[29]C. Cametti, P. Codastefano, P. Tartaglia, J. Rouch, and S. H. Chen, Phys. Rev. Lett. **64**, 1461 (1990).

[30]H. E. Roman, J. Stat. Phys. **58**, 375 (1990).

[31]R. M. Ziff and G. Stell (private communication).

[32]K. Golden, Phys. Rev. Lett. **65**, 2923 (1990).

[33]B. Mandelbrot, *Fractals: Form, Chance and Dimension* (Freeman, San Francisco, 1977).

[34]S. Alexander and R. Orbach, J. Phys. (Paris) Lett. **43**, L625 (1982).

[35]R. Rammal and G. Toulouse, J. Phys. (Paris) Lett. **44**, L13 (1983).

[36]A. U. Neumann and S. Havlin, J. Stat. Phys. **52**, 203 (1988).

[37]D. Y. Kim, H. J. Herrmann, and D. P. Landau, Phys. Rev. B **35**, 3661 (1987); I. Balberg, *ibid.* **37**, 2391 (1988).

[38]Z. Marohnic and E. Babic, in *Rapidly Quenched Metals,* edit-

ed by S. Steeb and H. Warlimont (Elsevier, Amsterdam, 1985), p. 1063.
[39]R. Reisser, M. Fähnle, and H. Kronmüller, J. Magn. Magn. Mater. **97**, 83 (1991).
[40]D. Drobac and Z. Marohnic, in *Rapidly Quenched Metals* (Ref. 38), p. 1133.
[41]P. Hargraves and R. A. Dunlap, J. Phys. F **18**, 553 (1988).
[42]A. Weinrib and B. I. Halperin, Phys. Rev. B **27**, 413 (1983).